WALAILAK JOURNAL
http://wjst.wu.ac.th Engineering and Physical Sciences

Experimental Study of a 2-stage Parabolic Dish-Stirling Engine in Thailand

Krissadang SOOKRAMOON[1,*], Pracha BUNYAWANICHAKUL[1] and Bancha KONGTRAGOOL[2]

[1]*Department of Mechanical Engineering, Faculty of Engineering, Srinakarinwirot University, Ongkharak, Nakhon Nayok 26120, Thailand*
[2]*Department of Energy Technology, Faculty of Engineering, North-Chiang Mai University, Hangdong, Chiang Mai 50230, Thailand*

([*]Corresponding author's e-mail: krissadangs@gmail.com)

Received: 25 December 2014, Revised: 14 May 2015, Accepted: 12 June 2015

Abstract

This paper conducted an experimental study of a laboratory-scaled 2-stage parabolic dish-Stirling engine. Experimental investigation of the system was performed, using an actual sun and a 2-stage parabolic dish concentrator as a heat source. Results from the performance testing by using a generator with a solar radiation and a double reflection parabolic dish solar concentrator in May 2014 indicated that the maximum concentrator efficiency is 26.291 %, the engine produced a maximum power of 0.359 W at 55.6 rpm, electrical power of 0.27 W, the generator efficiency at the maximum of 79.021 %, and the maximum overall brake thermal efficiency of 0.25033 %, approximately. The average heat input to concentrator is 1936.07 W and to the engine in an average of 180.28 W, respectively. The gross solar-to-electric conversion efficiency is 3.71 %.

Keywords: 2-stage parabolic dish, solar concentrator, solar-powered Stirling engine

Nomenclature

A_m	Aperture area of the main dish concentrator, m^2	P	Stirling engine power, W
A_s	Aperture area of the sub dish concentrator, m^2	P_G	The generator power output, W
$A_{2\text{-}Stage}$	Aperture area of 2-stage parabolic dish concentrator, m^2	Q_{con}	Total thermal energy come to a concentrator, W
A_H	Absorber area, m^2	q_A	The concentrated heat on the absorber plate, W
Cp	Specific heat of water at constant pressure, kJ kg^{-1} K^{-1}	q_{in}	The amount of heat absorbed by the water, W
$C_{1\text{-}stage}$	Main dish concentration ratio	q_s	Heat input from heat source for engine, W
$C_{2\text{-}stage}$	Sub dish concentration ratio	R_M	Main dish reflectivity , 0.8
D_m	Diameter of a main dish, m	R_S	Sub dish reflectivity, 0.95
D_s	Diameter of a sub dish, m	T_C	Engine cooler wall temperature, K
d_H	Absorber diameter, m		
E	Voltage reading from the meter, V	T_H	Engine heater wall temperature, K

E_{con}	Concentrator efficiency, %	T_m	The average temperature in the regenerator, K
E_{BT}	Brake thermal efficiency, %	$T_{w\ in}$	Inlet water temperature inside the receiver, K
E_O	The overall efficiency, %	$T_{w\ out}$	Outlet water temperature inside the receiver, K
F_1	Focal length of the main dish, m	t_1, t_2	Initial, final time of water temperature, °C
F_2	Focal length of the sub dish, m	W	Weight of mass, kg
h	Depth of the parabolic solar concentrator, m	*Greek symbols*	
h	Solar elevation angle, degree		
$I_{b,n}$	Direct solar radiation, W/m^2	η_{gen}	The generator efficiency, %
$I_{d,h}$	Diffuse solar radiation, W/ m^2	η_{gross}	The gross solar-to-electric conversion efficiency, %
$I_{t,h}$	Total solar radiation, W/m^2	θ_Z	solar azimuth angle, degree
m_w	Water mass flow rate, kg/s	δ	Declination angle, radian
N	Engine speed, rpm	ω	Hour angle, radian
P_B	The actual shaft power, W	φ	Altitude angle, radian

Introduction

The sun has an irradiance of about 63 MW/m^2. On the earth's surface, solar energy flow decreases down to approximately 1 kW/m^2. At the present time, solar energy is an eye-catching energy source, which can be used as a heat source for heat engines. The Stirling engine is a hot air engine, which works on a temperature differential, any heat source can be used to power the engine such as solar energy. In 1987, a solar powered Stirling engine was patented by Meijer [1] as shown in **Figure 1**. His innovation, a Stirling cycle engine, with a solar dish collector produces mechanical energy [2]. The output work of the Stirling cycle is then used to drive a generator and produce electric power. This apparatus reflects the sun rays into the focal point at the center of the paraboloidal dish. Solar energy is collected in the form of heat to power a Stirling cycle engine which operates by permitting heat flow from a hot source to a cold side in order to do work as shown in **Figure 1**. The dimensions of the Stirling engine can also be adjusted to advance the energy derived from the heat source. A Stirling engine uses the heated fluid to move pistons and create mechanical power. The mechanical work, in the form of the rotation of the engine's crankshaft, a Stirling engine requires an electric generator to transform its mechanical production into electricity.

In solar Dish-Stirling units, the solar energy is converted to electrical energy in 3 phases. In the first phase, radiation is converted to heat by concentrating the solar radiation onto a light absorbing heat pipe by means of a parabolic reflector. In the second phase, the heat is transformed into mechanical power by a Stirling engine. In the final phase, a generator converts the mechanical power to electricity. Generators fluctuating from low to high voltage outputs, alternating or direct current are available. Generators convert mechanical energy into electrical energy by using a center rotor that is bounded by stator magnets, which create a magnetic field. These rotors interrelate with either an electromagnet or a permanent magnet to generate electric current. The current that is formed can develop in either direct or alternating current.

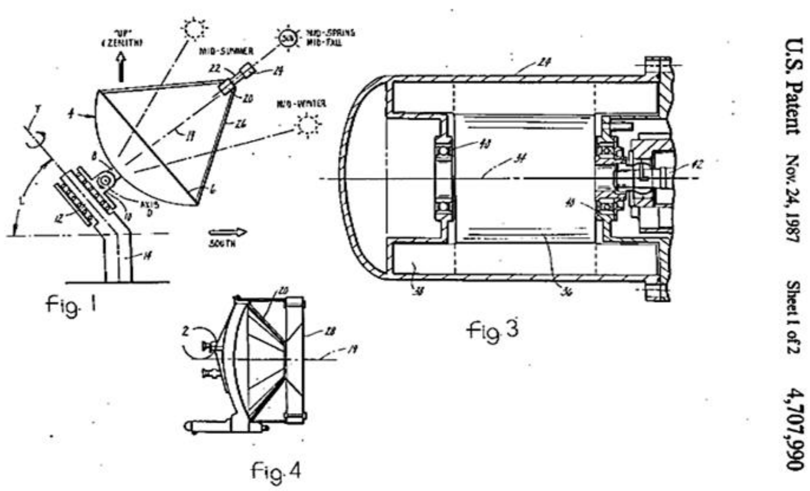

Figure 1 A solar powered Stirling engine by Meijer [1].

A rational amount of research work has been done to quantify and predict the performance of Stirling Engines and Concentrating Collector. In 1976, Pons and Fox [3] reported the use of heat pipe systems to run solar-powered Stirling engines and recommended some concepts of thermal storage. Even though this idea has merit, the increased complication may limit its use in technically untrained areas. In 1979, Holland [4] pointed out that the proper balancing of single cylinder Stirling engines was difficult, and may be solved by using relatively complex mechanisms, such as the Philips rhombic drive. Vibration is an important problem with solar-powered Stirling engines since they are generally mounted on light structures above parabolic dish collectors, and vibration of the dish would result in optical imprecision. In 1982, Leibowitz and Hanseth [5] presented the possibilities of Stirling engines working with high-temperature gas. However, with most improvements resulting from the use of sophisticated technology, rural areas of developing countries seem to not gain much from them. In 1983, efficiency is potentially high and Marriott [6] suggested an overall efficiency of 29 % before parasitic losses, and 26 % after deduction of all expected losses, for a 26.5 kW engine operated with a parabolic dish. In 1985, Selcuk and Bowyer [7] claimed a 32.5 % engine efficiency, with working fluid temperatures around 700 °C. Economic reflector design, to withstand the wind and weather, is important for this technology and continues to consume much effort. Lajet carried out a recent study, involving sophisticated wind-tunnel testing of loads on parabolic dish collectors. McGlaun [8] reported in 1987, that wind loading was much higher than predicted, and collector design changes are necessary. In 1987, Schlaich [9] developed a 17 m diameter dish, by using a sheet steel membrane formed into the reflecting surface shape by a partial vacuum. In 1987, 2 units of this design equipped with 50 kW Stirling engines were tested in Riyadh [10]. In 1990, Ahmed *et al*. [11] used a single membrane dish collector and hydrogen as an operational gas in the process of a 50 kW solar-powered Stirling engine electricity production. They described the problems of tracking system, due to errors in design and problems in starting during winter season, due to improper control part selection. In 1991, Kleih [12] proposed a Dish-Stirling test facility. The effects of the Stirling engine performance were collector geometry, insolation, and the engine configuration. Its performance from the test was in the range of 5 - 25 kWe. In 1999, Childs *et al*. [13] presented the innovative concept to determine the cost-effectiveness of new methodologies to solar powered desalting technology. Combined new solar conversion technology with lately advanced, hydraulic pump and energy regaining technology for solar desalting. A solar dish concentrator-Stirling engine, electric module with an overall efficiency of 22 % for 10 h/day average production, was reported. In 1999, Audy *et al*. [14] informed a Stirling engine for space station applications by using a solar dynamic power system. Theoretical models for dissimilar 4 representative orbit shapes were developed. The simulation consequences were compared to those of a solar dynamic power module, using a Brayton gas turbine. In 2007, Snidvongs [15] conducted a small solar dish Stirling engine 500 W stand-alone system with a medium insolation in Thailand. The 4-piston, double acting Gamma type solar Stirling engine was constructed and operated at 650 °C coupled with a 2.5 m diameter dish solar collector. The thermal efficiency was 60 % with a 31 % mechanical efficiency. In 2010, Wua *et al*. [16] proposed the thermal-electric conversion performance of parabolic dish/AMTEC solar thermal power system with an overall conversion efficiency of 20.6 % with an output power of 18.54 kW. In 2012, Ricardo [17] investigated a mathematical model for the study and design of a solar dish collector with cavity receiver for its application in a Stirling engine. This work suggested a mathematical model for the design of parabolic dish collector, with cavity receiver such as a Stirling engine, and analyzing the influence of geometric, operative and climatic variables on the efficiency and thermal capacity of the system. In 2013, Reddy *et al*. [18] studied the exergetic analysis and performance evaluation of parabolic dish Stirling engine solar power plant. A 50 MWe design capacity parabolic dish Stirling engine, solar power plant (PDSSPP) has been modeled for analysis, where 2000 units of a parabolic dish Stirling engine each having a capacity of 25 kWe were considered to get the desired capacity. An attempt has been made to carry out an energetic and exergetic analysis of the different components of a solar power plant system using parabolic dish collector/receiver and Stirling engine. The developed model was used in Jodhpur (26.29°N, 73.03°E) in India. It was found that year-round energetic efficiency varies from 15.57 to 27.09 %, and exergetic efficiency varies from 16.83 to 29.18 %. In 2014, Ahmadi *et al*. [19] reported a finite time thermodynamic (FTT) evaluation of a solar-dish Stirling heat engine. FTTs has been applied to decide the output power and the consistent thermal efficiency, exergetic efficiency, and the rate of entropy generation of a solar Stirling system with a finite rate of heat transfer, regenerative heat loss, conductive thermal connecting loss, and finite regeneration process time. The results imply that the optimized absorber temperature is somewhere between 850 and 1000 K. In 2014 Li *et al.* [20] conducted an adiabatic model of the Stirling engine developed for the study of a grid-connected dish-Stirling solar-thermal power plant. The model relates the average values of the engine state variables and also takes into description the engine losses. As the engine is shown to exhibit non-minimum phase behavior, an improved temperature control scheme for the engine heat absorber is developed. Containing the parameters such as engine speed, pressure, and solar insolation limits into the analysis, a steady-state feasible operating system of the solar-thermal power plant is obtained. The techniques of analysis for Stirling engines can be categorized with Martini's [21] classification as follows: 1) Zero the Order Analysis: as Beale formula. 2) First Order Analysis: (Schmidt analysis) was done in 1871 by Gustav Schmidt in which he obtained closed-form solutions for the special case of sinusoidal volume variations and isothermal hot and cold spaces. There are many ways to investigate the dish/Stirling performance and behavior, such as photometric, analytical and numerical. As the rationale mentioned above, there are no published papers on experimental studies of 2-stage dish Stirling engines. Thus, it is interesting to further study the 2-stage dish Stirling in detail.

This work deals with a calorimetric method to measure the heat gained from solar radiation, with a 2-stage parabolic dish concentrator to focus the hot end rod on the Stirling engine, then the engine produces mechanical energy which is transformed into electricity. A 2 axis sun tracking system was used to maintain the dish perpendicular to the sun. The performance of a 2-stage parabolic dish solar concentrator and Stirling engine were investigated as well. The laboratory scaled Stirling engine was kinematic; single acting one power piston, gamma configuration, using a non-pressurized air as a heat transfer fluid. The heat source used a 2-stage parabolic dish solar concentrator made from the satellite dish lined with aluminum foil reflector in stage one and a mini satellite dish lined with a light reflector sheet in stage 2, to reflect the Sun’s rays twice to maximize the thermal energy at the focal point of the system.

Materials and methods

Experimental apparatus

Solar-powered engine

The solar-powered Stirling engine was a single power piston, single acting configuration. The Displacer was made from an aluminum pipe. The purpose of this engine was to act as a laboratory-scale prototype engine for verification of actual solar-powered operations. This engine is experimented with actual solar energy, by using a 2-stage parabolic dish concentrator. The experiments consisted of using actual sun for heat input experiments and for engine performance experiments.

The main engine design parameters are listed in **Table 1**. It is designed as a single-acting, gamma-configuration with a power piston. The power cylinders are directly connected to the cooler plate, to minimize the cold space and transfer port dead volume. A photograph of this engine is shown in **Figure 2**.

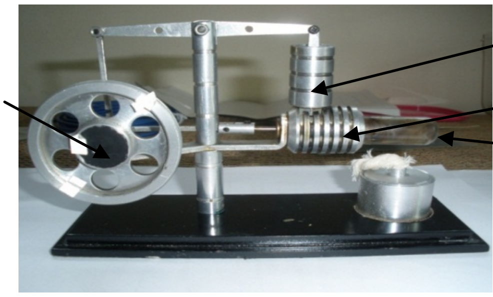

Figure 2 The solar-powered engine.

Table 1 Solar-powered engine main design parameters.

Stirling engine configuration: Gamma		Size
Power piston:	bore × stroke (mm)	12.0 × 3.0
Swept volume (cc)		0.339
Displacer:	bore × stroke (mm)	9 × 6.2
Swept volume (cc)		0.394
Compression ratio		4.94
Phase angle		90^o

A 2-stage concentration parabolic dish

The apparatus consists of paraboloidal dishes made of different type of materials and reflectors. The main dish is fabricated using a 1.68 m diameter satellite dish with a 0.741 m focal length. The sub dish was 0.625 m diameter mini satellite dish with a 0.632 m focal length of the secondary stage. The reflecting surface was covered with aluminum sheet lining and lighting reflector for the main dish and sub dish, respectively. The design parameters are shown in **Table 2** and the configuration is shown in **Figure 3** below. Two dishes are supported by a high-strength frame equipped with a 2-axis sun tracking system. The aims of the 2-stage concentration parabolic dish are to boost the concentration ratio, which increases the heat flux of solar radiation.

Table 2 A 2-stage concentration parabolic dish main design parameters.

Symbol	Dimension	Symbol	Dimension
A main dish (m^2)	2.216	D_{main} (m)	1.68
A sub dish (m^2)	0.309	d_H (mm)	138
A_H (m^2)	0.014957	F_1 (mm)	672
$A_{2\text{-stage}}$ (m^2)	1.9064	F_2 (mm)	632
$C_{1st.}$	127.459	$Q_{con\ in}$ average (W)	1936.07
$C_{2st.}$	254.918		

The experimental set up

The experimental setup consists of the calorimeter, the engine coupled to a generator, solar radiation measuring equipment, thermocouple, data acquisition system and a double reflection parabolic dish concentrator as shown in **Figures 3** and **4**.

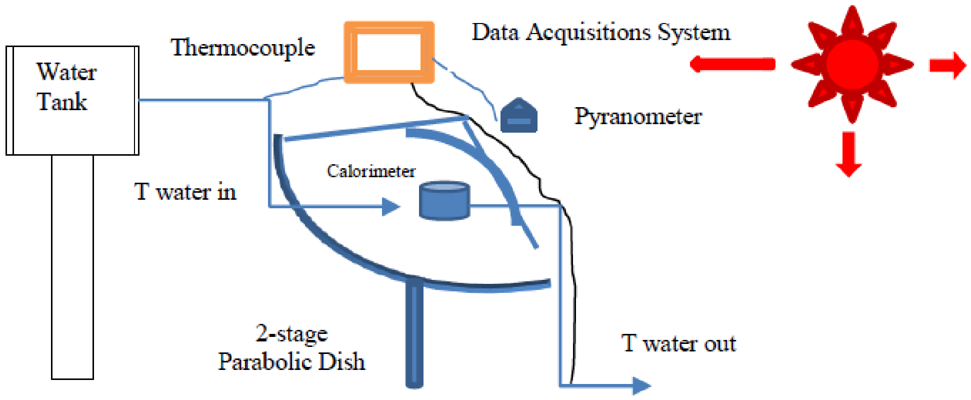

Figure 3 Schematic diagram of heat input experiment.

Figure 4 The simple calorimeter with a 2-stage concentration parabolic dish experimental setup.

The cooling air is supplied by air passing through the fins. The cooler temperature, T_C and the heater temperature, T_H, are measured by infrared thermocouples. The temperature indicators are shown in **Figure 5**.

Figure 5 A simple calorimeter for engine heat input experiment and data logger.

The displacer cylinder is used as a flowing calorimeter as shown in **Figure 5**. The constant water flow is provided by the constant head of the water storage tank. The water flow rate is measured by using a beaker and a stopwatch. The water inlet and outlet temperature are measured using K-type thermocouples and recorded in a data logger. The diffuse intensity on a horizontal plane ($I_{d,\ h}$), is measured by using a pyranometer (CM 11 Kipp & Zonnen, 5.67 μV/W/m^2) and a shading ring. The solar zenith angle is measured as well. The apparatus setup for the engine–generator output experiment is shown in **Figures 6 - 8**. The solar total intensities in the horizontal plane ($I_{t,\ h}$) are measured by a pyranometer and recorded in Graphtec data logger model GL820 as shown in **Figure 5**. The generator is driven by an engine via a rubber belt, as shown in **Figure 7**. The small DC lamps are used as a load for the generator, as shown in **Figures 9 - 10**.

Figure 6 The temperature indicators measuring instrument.

Figure 7 The concentrator experiment arrangement.

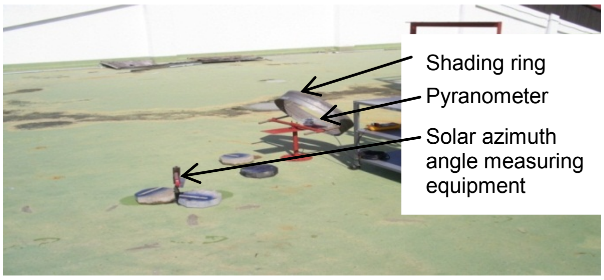

Figure 8 The shading ring and equipment for solar zenith angle measurement.

Figure 9 The apparatus arrangement for the engine-generator output experiment.

Figure 10 The measuring instrument for the engine-generator output experiment.

Experimental procedure

The performance study of the laboratory-scale single-acting gamma-configuration Stirling engine equipped with a 2-stage parabolic dish solar concentrator to concentrate solar radiation to its focal point as a heat source.

The details of the experimental work consist of the following steps:

Experiment 1 A 2-Stage parabolic dish solar concentrator with a simple calorimeter

The concentrator experiment is done; the objective of the concentrator experiment is to determine the actual heat input into the engine. The solar concentrator reflects solar radiation twice for increasing the concentration ratio to the calorimeter, which is placed at its focal point and represented to the engine displacer. The flowing water with a mass flow rate of 1.33 g/s from the water storage tank flows through the calorimeter (in a size of 138 mm diameter copper made) to absorb this heat.

The heat input into a simple calorimeter can be determined from;

$$q_{in} = m_w c_p (T_{w,out} - T_{w,in}) \quad (1)$$

Experiment 2 The engine experiment with a 2-stage parabolic dish solar concentrator

For the engine experiment with the sun, the concentrated heat flux was placed underneath the displacer head. The displacer head was heated up by the concentrated heat flux until it reached the operating temperature. The engine is then started and run, until steady state conditions were reached. The engine was loaded by adding a weight to the rope brake dynamometer. Then, the speed reading, spring balance reading and all temperatures from thermocouples were recorded. Another vary loading weight was added to the dynamometer until the engine stopped.

The direct solar intensity on the normal plane can be calculated from;

$$I_{b,n} = (I_{t,h} - I_{d,h})/\cos\theta_z \quad (2)$$

For an absorber having an area A, with the intensity of solar radiation of $I_{b,n}$, the concentrated heat on the absorber plate may be calculated from;

$$q_A = I_{b,n} A_H \quad (3)$$

where I_S is the concentrated intensity on an absorber plate and is equal to the average intensity, and A_H is the absorber area. The absorber diameter is 138 mm.

The useful heat input is the amount of heat absorbed by the water inside the calorimeter, and can be determined from;

$$q_{in} = m_w c_p \frac{\Delta T}{\Delta t} \quad (4)$$

where m_w is water mass (1.5 kg), c_p is a specific heat at constant inlet water temperature, (4168 J/kg K) [22], ΔT is the water temperature rise, Δt is the time taken during the water temperature rise.

Experiment 3 Engine performance experiment

The engine performance, experimental results are shown in **Table 3**. In these tables, the engine torque is calculated from;

$$M_t = (S-G)\, r \quad (5)$$

where S is the spring balance reading (N), and G is the loading weight (N), and r is the brake drum radius

The actual shaft power can be calculated from;

$$P_B = 2\pi\, M_t\, n \quad (6)$$

where n is the engine speed (rps).

E_{BT} is the brake thermal efficiency, calculated from;

$$E_{BT} = P_B/q_S \quad (7)$$

where q_S is the heat input from the heat source to the engine.

The total solar energy coming to the concentrator may be calculated from the equation, as follows;

$$Q_{con} = R_m \times R_s \times I_{b,n} \times A_{2\text{-}stage} \quad (8)$$

This applies when R_m is the reflectivity of the main dish reflector surface and R_s is the reflectivity of the sub dish reflector surface. $I_{b,n}$ is the direct solar intensity on the normal plane and $A_{2\text{-}stage}$ is the total aperture area of the system.

The concentrator efficiency can be calculated from the useful heat input to the calorimeter and the total energy coming to the concentrator, as follows;

$$E_{con} = q_{in} / Q_{con}$$

$$= q_{in} / R_m \times R_s \times I_{b,n} \times A_{2\text{-}stage} \quad (9)$$

The generator power output and efficiency

The engine-generator power output experiment is carried out to determine the power output from the engine-generator set. The load on the generator is measured by using a load bank, voltmeter and ammeter. The generator power output is calculated from;

$$P_G = I\, E \quad (10)$$

where I (A) and E (V) is reading from the meter.

The generator efficiency can be calculated from;

$$\eta_{gen} = P_G/P_B \tag{11}$$

The gross solar-to-electric conversion efficiency is the product of Eqs. (7), (9) and (11);

$$\eta_{gross} = E_{BT}\, E_{con}\, \eta_{gen} \tag{12}$$

Solar tracking system

A 2-stage parabolic dish Stirling engine with automatic 2 axes sun tracking system was used to track the sun. The system consists of electro-optic part represented by photo sensors by using 4 LDR placed in the 4 corners of the main dish, two 12V DC motors and an electronic control box. The 2 important solar angles are as follows:

Solar azimuth angle

For a fixed point on the earth's surface (for a specific longitude and altitude) the sun begins a move from east to west. This is the angle between the line that points to the sun and south. The angle is negative to the east and positive to the west. This angle is 0° at noon. It is probably close to −90° at sunrise and 90° at sunset, depending on the season. The azimuth angle is calculated according to the following equation;

$$\sin \theta_Z = \frac{\cos\delta \sin\omega}{\cos h} \tag{13}$$

Solar elevation angle

The solar elevation angle is the angle between the line that points to the sun and the horizontal. It is the complement of the zenith angle. This angle is 0° at sunrise and sunset. The elevation angle is calculated as follows;

$$\sin h = \cos \varphi \cos\delta \cos \omega + \sin\varphi \sin\delta \tag{14}$$

Results and discussion

A 2-stage parabolic dish solar concentrator with a simple calorimeter

The actual heat input to the engine q_{in}, from the solar radiation heat flux, was experimentally determined, by using flowing calorimeter to measure the absorbed heat. The actual heat input to the engine and the heat source efficiency, the variations in heat source efficiency with an average intensity on the concentrator, is shown in **Table 3** and **Figure 11**. It can be seen that the concentrator efficiency increases as the average intensity increases.

Table 3 A 2-stage parabolic dish solar concentrator experiment.

No.	Time	Water temp.		θ_Z	$I_{t,h}$	$I_{d,h}$	$I_{b,n}$	Q_{in}	$Q_{absorbed}$	Econ
		Inlet °C	Outlet °C	deg.	W/m^2	W/m^2	W/m^2	W	W	%
1.00	7:30			-68.76	253.59	44.00	578.54	838.23		
2.00	7:45			-69.20	253.59	84.00	477.58	691.95		
3.00	8:00			-70.79	338.12	83.00	775.38	1123.42		
4.00	8:15			-71.06	380.39	83.00	916.23	1327.50		
5.00	8:30			-71.33	422.65	83.00	1061.03	1537.29		
6.00	8:45			-71.60	507.19	83.00	1343.85	1947.06		
7.00	9:00			-72.58	549.45	83.00	1558.09	2257.46		
8.00	9:15			-72.66	591.72	83.00	1706.86	2473.01		
9.00	9:30			-72.73	676.25	83.00	1998.31	2895.27		
10.00	9:45			-72.81	718.51	83.00	2150.33	3115.54		
11.00	10:00			-73.09	760.78	83.00	2330.18	3376.11		
12.00	10:15	34.00	37.00	-72.84	803.04	83.00	2440.48	3535.93	16.71	0.47
13.00	10:30	34.00	43.00	-72.60	803.04	83.00	2407.84	3488.64	50.12	1.44
14.00	10:45	34.00	51.00	-72.35	845.31	125.00	2375.68	3442.03	94.66	2.75
15.00	11:00	34.00	53.00	-71.44	887.57	86.00	2518.32	3648.70	105.80	2.90
16.00	11:15	34.00	57.30	-70.29	870.00	126.00	2206.02	3196.22	129.75	4.06
17.00	11:30	34.00	85.60	-69.15	966.00	126.00	2360.06	3419.41	287.33	8.40
18.00	11:45	34.00	81.20	-68.00	975.00	126.00	2266.38	3283.67	262.83	8.00
19.00	12:00	34.00	95.60	-63.80	974.00	158.00	1848.22	2677.82	343.02	12.81
20.00	12:15	34.00	93.00	-57.89	969.00	161.00	1520.09	2202.41	328.54	14.92
21.00	12:30	34.00	91.00	-51.98	946.00	123.00	1336.18	1935.94	317.40	16.40
22.00	12:45	34.00	87.00	-46.07	952.00	167.00	1131.48	1639.37	295.13	18.00
23.00	13:00	35.00	93.50	-24.40	945.00	165.00	856.50	1240.95	325.76	26.25
24.00	13:15	35.00	95.30	-30.31	961.00	200.00	881.49	1277.16	335.78	26.29
25.00	13:30	36.00	87.00	-36.22	972.10	167.00	997.96	1445.90	283.99	19.64
26.00	13:45	35.00	87.00	-42.13	972.10	200.00	1041.10	1508.41	289.56	19.20
27.00	14:00	35.00	88.00	63.80	929.84	230.00	1585.12	2296.62	295.13	12.85
28.00	14:15	35.00	81.00	64.95	820.00	240.00	1369.83	1984.70	256.15	12.91
29.00	14:30	34.00	77.00	66.09	700.00	242.00	1130.02	1637.25	239.45	14.62
30.00	14:45	33.00	63.00	67.24	718.51	243.00	1229.12	1780.83	167.05	9.38
31.00	15:00	33.00	55.00	71.44	464.92	159.00	961.11	1392.52	122.51	8.80
32.00	15:15	33.00	51.00	71.69	422.65	121.00	960.20	1391.20	100.23	7.20
33.00	15:30	33.00	48.00	71.94	380.39	121.00	836.70	1212.27	83.53	6.89
34.00	15:45	33.00	47.00	72.18	338.12	121.00	709.49	1027.95	77.96	7.58
35.00	16:00	33.00	43.00	73.09	253.59	121.00	455.85	660.46	55.68	8.43
36.00	16:15	33.00	44.00	73.01	295.86	121.00	598.41	867.01	61.25	7.06
37.00	16:30	33.00	43.00	72.94	253.59	121.00	451.96	654.83	55.68	8.50
38.00	16:45	33.00	39.00	72.86	211.33	78.00	452.40	655.47	33.41	5.10
39.00	17:00	33.00	39.00	72.58	126.80	40.00	289.93	420.06	33.41	7.95
Average		33.89	66.27		646.39	126.38	1336.27	1936.07	180.28	9.31

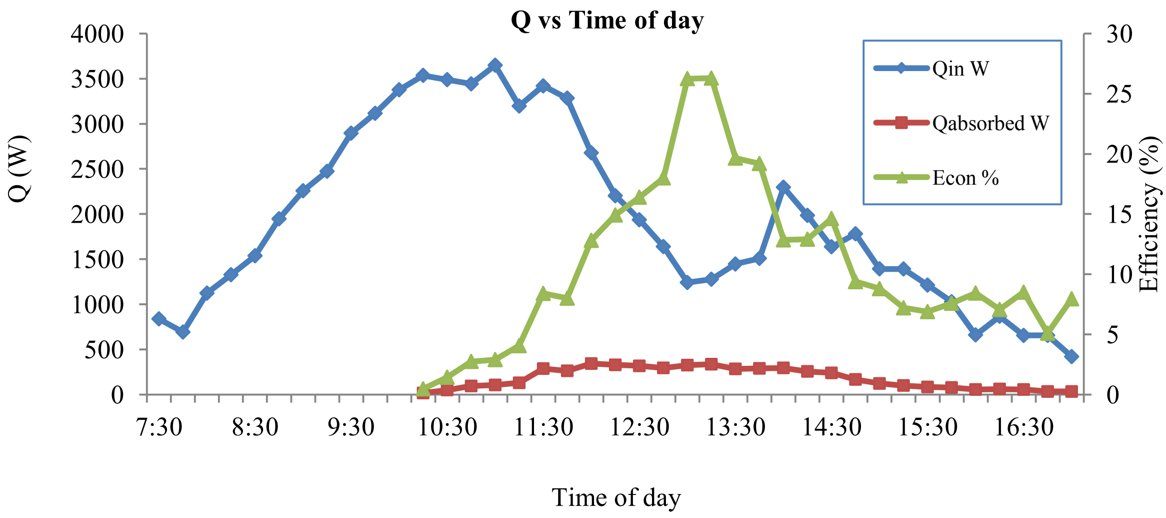

Figure 11 Results from the heat source experiment, using a simple calorimeter.

Engine Experiment with a 2-Stage Parabolic Dish Solar Concentrator

From the experimental results, the engine started up at an initial temperature of 250 °C and came to steady state running between 250 - 260 °C and is the maximum power of the engine.

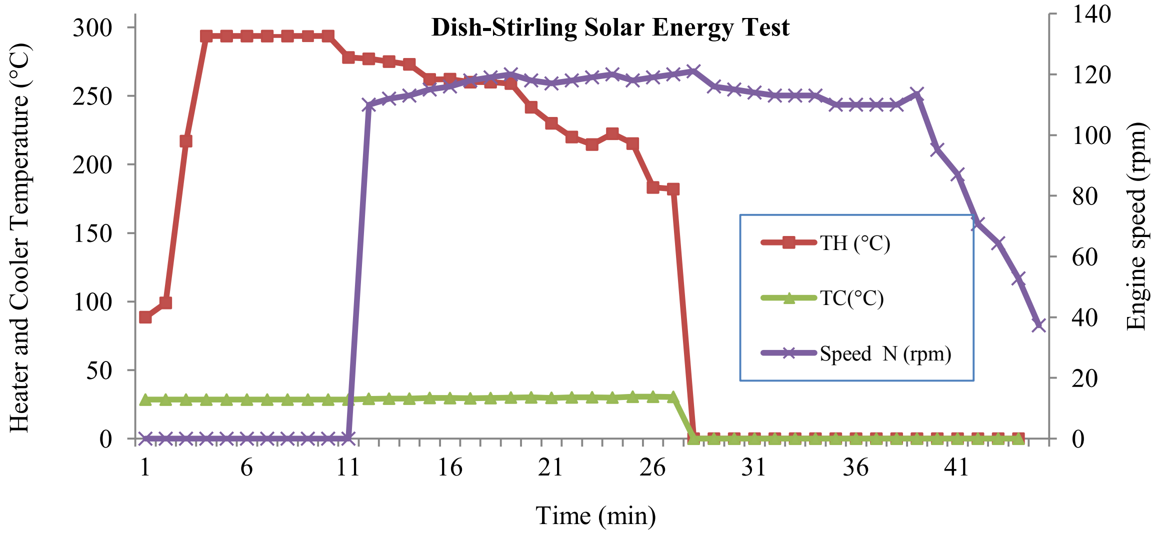

Figure 12 Results of the solar test: gamma-type Dish-Stirling engine.

Engine performance experiment

The engine performance, on average, at solar intensities of 870 - 961 W/m^2, the variations in the engine torque, shaft power, and brake thermal efficiency, at the variation of solar intensity with engine speed are shown in **Figure 13**. As expected, the best engine performance results from the higher heat input. An increase in the engine torque, shaft power and brake thermal efficiency, is shown to also depend on the heater temperature. The values for maximum torque, shaft power and brake thermal efficiency are summarized in **Table 4**. The maximum shaft power and heater temperature, at various heat inputs, the shaft power and heater temperature increases as a function of the average intensity. Therefore, greater shaft power will be obtained from the higher average intensity. **Figure 13** also shows the variations in brake thermal efficiency, heat source efficiency and overall efficiency with the average intensity. It can be seen that brake thermal and overall efficiency increase, as the average intensity rises.

Table 4 Performance of the dish-Stirling engine.

N (rpm)	S (kg)	W (kg)	T (N.m)	P (W)	V	A	P_G (W)	E_{BT} (%)	E_O (%)	η_{gen} (%)	E_{con} (%)	η_{gross} (%)
55.600	0.007	0.074	0.062	0.359	1.180	0.230	0.271	0.250	0.006	75.531	14.910	2.819
48.150	0.009	0.084	0.069	0.348	1.120	0.230	0.258	0.243	0.001	73.929	16.390	2.941
39.850	0.010	0.094	0.077	0.323	1.110	0.230	0.255	0.225	0.001	79.021	18.000	3.201
39.200	0.010	0.094	0.077	0.317	0.980	0.230	0.225	0.324	0.000	71.093	26.250	6.040
31.500	0.001	0.034	0.030	0.101	0.870	0.103	0.090	0.128	0.000	89.492	26.290	3.023
						Ave.	0.220	0.234	0.002	77.813	20.368	3.710

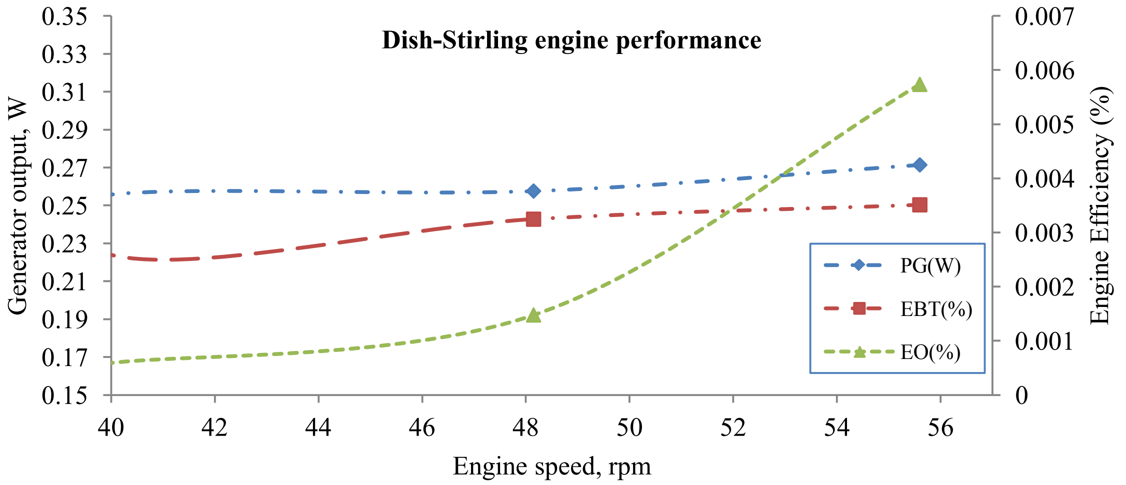

Figure 13 Results of the dish-Stirling power generation.

The relationship between the torque and speed are shown in **Table 4** and the generator power output versus speed shows a maximum power of 0.27 W at 55.6 rpm.

Conclusions

In this study, a laboratory-scale parabolic dish-Stirling engine, with a 2 axis sun tracking system has been experimentally investigated, using an actual sun and a 2-stage parabolic dish concentrator as a heat source. The actual heat input to the dish-Stirling engine was measured at different water temperatures and assessed by the calorimetric method. The thermal efficiency of the concentrator depends on the absorbed heat capability of the receiver, solar intensity and total aperture area of the dish. From the experiment, the maximum concentrator efficiency was found near 1 p.m. to be around 26.29 % because of the incoming solar radiation on that day gave more direct solar radiation. Although the performance of the system is not so high, this study shows promise in concentrating solar power technology. This information can be used for consideration in the large scale construction of solar dish power generation development in remote areas in the near future. To increase the efficiency of the system we recommend:

- Better quality materials for the main dish and light reflector to achieve higher reflectivity, advanced thermal efficiency can be reached.
- Enlarge the main dish and sub dish to increase the aperture area to add more heat input.
- Enhance the brake power of the Stirling engine by scaling up the size of the engine. Increase the hot end of the engine and add more fins to the heat sink for increase the cooling.
- The shading of the sub dish blocked solar radiation onto a main dish reduces total aperture area. Redesign the sub dish in another form such as a hyperbolic shape.
- Scale up of the system could be done after the study to detail heat loss from the receiver of the Stirling engine such as convection and radiation loss. Minimizing heat loss would gain more useful heat, which would be transferred to the engine.

Acknowledgements

The authors would like to express thanks to Srinakarinwirot University colleagues for the useful advice and gratefully thank the Department of Energy Policy and Planning Organization Thailand for providing financial support for this research work.

References

[1] JR Meijer. 1987, Solar Powered Stirling Engines. U.S. Patent 4,707,990.
[2] MJ Michael and NJ Hoboken. *Fundamentals of Engineering Thermodynamics*. John Wiley & Sons, New York, 2011, p. 72-3.
[3] RL Pons and RJ Fox. A solar/Stirling total energy system. *In*: Proceedings of the Sharing the Sun, Solar Technology in the Seventies Conference, Winnipeg, Canada, 1976, p. 77-91.
[4] MB Holland. The Stirling engine- power plant of the future. *Charter. Mech. Eng.* 1979; **26**, 60-3.
[5] L Leibowitz and E Hanseth. Solar thermal technology-outlook the 80's. *Mech. Eng.* 1982; **104**, 30-5.
[6] AT Marriott. Solar electric power from parabolic dishes. *In*: Proceedings of the Solar World Congress, Perth, Australia, 1983, p. 1438-43.
[7] MK Selcuk and JM Bowyer. Dish Stirling module performance analysis as evaluated from tests of various TBC concentrator / USAB engine configurations as the parabolic dish test site. *Ext. Abst. Intersol.* 1985, 313.
[8] MA McGlaun. The LaJet energy large scale innovative solar concentrator study of wind loading effects. *Abs. ISES Solar World Cong.* 1987; **2**, 15.
[9] J Schlaich. Solar power plants with a membrane concave mirror-50 kW. *Abs. ISES Solar World Cong.* 1987; **2**, 18.
[10] A Al-Rebaian and J Hansen. 50 kW solar concentrators with Stirling generators-results of the first six mounts of operation in Saudi Arabia. *Abs. ISES Solar World Cong.* 1987; **2**, 13.
[11] A Ahmed, M Al-Agami and M Al-Garni. Solar powered Stirling engine with a single membrane dish concentrator. *In*: Proceedings of the 1st World Renewable Energy Congress, Energy and The Environment, Reading, UK, 1990; **2**, 1202-7.

[12] J Kleih. Dish-Stirling test facility. *Sol. Energ. Mater*. 1991; **67**, 317-30.
[13] WD Childs, AE Dabiri, HA Al-Hinai and A Havari-Ro. Solar-powered desalting technology. *Desalination* 1999; **125**, 155-66.
[14] Ch Audy, M Fischer and EW Messerschmid. Nonsteady behavior of solar dynamic power systems with Stirling cycle for space stations. *Aerosp. Sci. Tech*. 1999; **1**, 49-58.
[15] S Snidvongs and S Chindaraksa. The design of a small solar thermal dish Stirling 500 W stand alone in Thailand. *In*: Proceedings of the Energy Sustainability 2007, Longbeach, USA, 2007, p. 27-30.
[16] W Sy, L Xiao, Y Cao and YR Li. A parabolic dish/AMTEC Solar thermal power system and its performance evaluation. *J. Appl. Energ*. 2010; **87**, 452-62.
[17] R Beltran, N Velazquez, AC Espericueta, D Sauceda and G Perez. Mathematical model for the study and design of a solar dish collector with cavity receiver for its application in Stirling engines. *J. Mech. Sci. Tech*. 2012; **26**, 3311-21.
[18] VS Reddy, SC Kaushik and SK Tyagi. Exergetic analysis and performance evaluation of parabolic dish Stirling engine solar power plant. *Int. J. Energ. Res*. 2013; **37**, 1287-301.
[19] HM Ahmadi, H Sayyaadi and H Hosseinzadeh. Optimization of output power and thermal efficiency of solar-dish Stirling engine using finite time thermodynamic analysis. *Int. J. Energ. Res*. 2014; **37**, 1287-301.
[20] Y Li, SS Choi and C2 Yang. Dish-Stirling solar power plants: Modeling, analysis, and control of receiver temperature. *IEEE Trans. Sustain. Energ.* 2014; **5**, 398-407.
[21] RW Dyson, SD Wilson and CT Roy. Review of computational Stirling analysis methods. *In*: Proceedings of the 2nd International Energy Conversion Engineering Conference, American Institute of Aeronautics and Astronautics Providence, Rhode Island, 2004, p. 1-10.
[22] European Standard. *Domestic Cooking Appliances Burning Gas*. 2nd ed. EN 30, 1979.